

1 **The Vitamin D Receptor (VDR) Regulates Mitochondrial Function in C2C12**  
2 **Myoblasts**

3

4 Stephen P. Ashcroft<sup>1</sup>, Joseph J. Bass<sup>2</sup>, Abid A. Kazi<sup>3</sup>, Philip J. Atherton<sup>2</sup>, Andrew  
5 Philp<sup>1,4,5</sup>

6

7 <sup>1</sup>School of Sport, Exercise and Rehabilitation Sciences, University of Birmingham,  
8 Birmingham, UK.

9 <sup>2</sup>MRC-ARUK Centre for Musculoskeletal Ageing Research, Clinical, Metabolic and  
10 Molecular Physiology, University of Nottingham, Royal Derby Hospital Centre,  
11 Derby, UK.

12 <sup>3</sup>Department of Cellular and Molecular Physiology, Pennsylvania State University  
13 College of Medicine, Hershey, Pennsylvania, USA.

14 <sup>4</sup>Mitochondrial Metabolism and Ageing Laboratory, Garvan Institute of Medical  
15 Research, Sydney, NSW, 2010, Australia.

16 <sup>5</sup>St Vincent's Clinical School, UNSW Medicine, UNSW Sydney, NSW, 2010,  
17 Australia.

18

19 **Running Title: Vitamin D Receptor and Mitochondrial Function**

20 **Word Count: 3956 (4000 limit)**

21 **Correspondence:**

22 Dr Andrew Philp

23 Mitochondrial Metabolism and Ageing Laboratory

24 Healthy Ageing Theme

25 Garvan Institute of Medical Research

26 384 Victoria Street, Darlinghurst, Sydney, NSW, 2010, Australia

27 Email: [a.philp@garvan.org.au](mailto:a.philp@garvan.org.au)

28 **ABSTRACT**

29 Vitamin D deficiency has been linked to a reduction in skeletal muscle function and  
30 oxidative capacity however, the mechanistic basis of these impairments are poorly  
31 understood. The biological actions of vitamin D are carried out via the binding of  
32  $1\alpha,25\text{-dihydroxyvitamin D}_3$  ( $1\alpha,25(\text{OH})_2\text{D}_3$ ) to the vitamin D receptor (VDR). Recent  
33 evidence has linked  $1\alpha,25(\text{OH})_2\text{D}_3$  to the regulation of skeletal muscle mitochondrial  
34 function *in vitro* however, little is known with regard to the role of the VDR in this  
35 process. To examine the regulatory role of the VDR in skeletal muscle mitochondrial  
36 function, we utilised lentiviral mediated shRNA silencing of the VDR in C2C12  
37 myoblasts (VDR-KD) and examined mitochondrial respiration and protein content  
38 compared to shRNA scrambled control. VDR protein content was reduced by ~95%  
39 in myoblasts and myotubes ( $P < 0.001$ ). VDR-KD myoblasts displayed a 30%, 30%  
40 and 36% reduction in basal, coupled and maximal respiration respectively ( $P < 0.05$ ).  
41 This phenotype was maintained in VDR-KD myotubes, displaying a 34%, 33% and  
42 48% reduction in basal, coupled and maximal respiration ( $P < 0.05$ ). Furthermore,  
43 ATP production derived from oxidative phosphorylation ( $\text{ATP}_{\text{Ox}}$ ) was reduced by  
44 20% suggesting intrinsic impairments within the mitochondria following VDR-KD.  
45 However, despite the observed functional decrements, mitochondrial protein content  
46 as well as markers of mitochondrial fission were unchanged. In summary, we  
47 highlight a direct role for the VDR in regulating skeletal muscle mitochondrial  
48 respiration *in vitro*, providing a potential mechanism as to how vitamin D deficiency  
49 might impact upon skeletal muscle oxidative capacity.

50

51 **Word Count: 245 (250 limit)**

52

53

## 54 INTRODUCTION

55

56 Vitamin D deficiency is characterised by serum 25-hydroxyvitamin D (25(OH)D)  
57 levels of  $<50 \text{ nmol.L}^{-1}$  (15). Based upon these numbers, it has been reported that  
58 approximately 40% of adults in the USA can be classified as deficient (7). The  
59 classical actions of vitamin D are well established, primarily functioning to maintain  
60 calcium and phosphate balance in order to prevent bone related disease (1, 13).  
61 Vitamin D carries out its actions via its active metabolite,  $1\alpha,25\text{-dihydroxyvitamin D}_3$   
62 ( $1\alpha,25(\text{OH})_2\text{D}_3$ ), which binds to the ubiquitously expressed vitamin D receptor (VDR)  
63 (14). The VDR, together with its binding partner retinoid x receptor alpha ( $\text{RXR}\alpha$ ),  
64 recruit transcriptional cofactors to regulate genomic transcription (17, 21).

65

66 In addition to its role in bone biology, vitamin D has also been shown to play a role in  
67 skeletal muscle development (11, 20) and regeneration (20). Given that vitamin D  
68 exerts its biological actions through binding to the VDR, multiple studies have sought  
69 to elucidate the role of the VDR within skeletal muscle (9, 10, 12). For example,  
70 whole body VDR knock-out mice (VDRKO) present muscle weakness, muscle fibre  
71 atrophy and hyper-nuclearity (8), which is also present in skeletal muscle-specific  
72 VDR knock-out (VDR-mKO) mice (9). Collectively these studies suggest a specific  
73 role for the VDR in skeletal muscle regulation (4, 10).

74

75 In addition to regulating skeletal muscle mass and function, evidence also suggests  
76 that vitamin D may regulate skeletal muscle mitochondrial function (2, 26). For  
77 example, treating human primary myoblasts with  $1\alpha,25(\text{OH})_2\text{D}_3$  resulted in an  
78 improvement in mitochondrial function and an increase in ~80 mRNAs encoding for

mitochondrial proteins (23). In addition, the VDR appeared to be critical in mediating the effects of  $1\alpha,25(\text{OH})_2\text{D}_3$ , as siRNA targeted towards the VDR blocked mitochondrial adaptation. Therefore, the aim of the present work was to further examine the regulatory role of the VDR for mitochondrial function in skeletal muscle. To achieve this, we generated a stable VDR loss-of-function C2C12 cell line model and examined mitochondrial respiration and protein content in myoblasts and fully differentiated myotubes.

86

## 87 **METHODS**

88

### 89 **Generation of VDR-KD and control cell lines**

90 The lentiviral plasmid used (pLKO.1 backbone) was designed in-house and was  
91 based on (Clone ID: RMM3981-201757375) and targeted the (3' UTR) mouse  
92 sequence 5'- TTA AAT GTG ATT GAT CTC AGG-3' of the mouse *Vdr* gene; the  
93 scramble shRNA was used as a negative control as previously reported (16) with a  
94 hairpin sequence: CCT AAG GTT AAG TCG CCC TCG CTC TAG CGA GGG CGA  
95 CTT AAC CTT AGG (Addgene plasmid 1864, Cambridge, MA, USA). Oligos were  
96 obtained from ITDDNA USA (Integrated DNA Technologies, Inc. Iowa, USA) and  
97 suspended, annealed and cloned into pLKO.1 at EcoRI and AgeI restriction sites as  
98 per the pLKO.1 protocol from Addgene. The resultant plasmids were transformed in  
99 DH5 $\alpha$  cells for amplification and isolated. The actual DNA sequence was confirmed  
100 at the Pennsylvania State University College of Medicine DNA sequence core  
101 facility. Packaging plasmids psPAX2 and envelope protein plasmid pMD2.G were a  
102 gift from Prof. Didier Trono, available as Addgene plasmids 12260 and 12259  
103 respectively. HEK293FT cells (Invitrogen, Carlsbad, CA, USA) were grown in

DMEM; 80–85% confluent plates were rinsed once with Opti-MEM (Invitrogen, Carlsbad, CA, USA) and then incubated with Opti-MEM for 4 h before transfections. psPAX2 and pMD2.G along with either scramble or pLKO.1 clones targeting mouse Vdr. Three clones were added after mixing with Lipofectamine 2000 as per the manufacturer's instructions (Invitrogen, Carlsbad, CA, USA). Opti-MEM was changed after overnight incubation with DMEM containing 10% fetal bovine serum (FBS) without antibiotics to allow cells to take up the plasmids and recover. Culture media were collected at 36 and 72 h post-transfection for viral particles. Viral particles present in the supernatant were harvested after a 15-minute spin at 1,500 *g* to remove cellular debris. The supernatant was further filtered using a 0.45- $\mu$ m syringe filter. Supernatant-containing virus was either stored at  $-80^{\circ}\text{C}$  for long-term storage or at  $4^{\circ}\text{C}$  for immediate use. C2C12 myoblasts (ATCC, Virginia, USA) at 60% confluence were infected twice overnight with 3 ml of viral supernatant containing  $8\text{ }\mu\text{g.ml}^{-1}$  polybrene in serum-free–antibiotic-free DMEM. Fresh DMEM media containing 10% FBS, 1% penicillin-streptomycin and  $2\text{ }\mu\text{g.ml}^{-1}$  puromycin dihydrochloride (Sigma, St. Louis, MO, USA) were added the next day. Cells that survived under puromycin selection were harvested as stable VDR knock-down (VDR-KD) myoblasts or controls and stored in liquid  $\text{N}_2$  until further analysis.

### **Extracellular flux analysis**

Both control and VDR-KD ( $n=9\text{--}10$  wells/group) cells were seeded in XF24-well cell culture microplates (Seahorse Bioscience, North Billerica, MA, USA) at  $3.0 \times 10^5$  cells/well in 100  $\mu$ l of growth medium. For myoblast experiments, cells were incubated at  $37^{\circ}\text{C}$  and 5%  $\text{CO}_2$  for 3 h in order to allow sufficient time for adherence and subsequently assayed. For myotube experiments, cells were incubated for a

period of 24 h and medium changed to differentiation medium (DMEM, 2% horse serum and 1% penicillin-streptomycin). Differentiation media was changed every other day for 7 days. Prior to the assay, cells were washed and placed in 500 µl of Seahorse XF Base Medium (glucose 10 mM, sodium pyruvate 1 mM, glutamine 1 mM, pH 7.4) pre-warmed to 37°C. The plate was then transferred to a non-CO<sub>2</sub> incubator for 1 h. Following calibration, cell respiratory control and associated extracellular acidification were assessed following the sequential addition of oligomycin (1 µM), carbonyl cyanide *p*-trifluoromethoxyphenylhydrazone (1 µM) and a combination of antimycin A and rotenone (1 µM). Upon completion of the assay, cells were collected in sucrose lysis buffer (50 mM Tris pH 7.5; 270 mM sucrose; 1 mM EDTA; 1 mM EGTA; 1% Triton X-100; 50 mM sodium fluoride; 5 mM sodium pyrophosphate decahydrate; 25 mM beta-glycerolphosphate; 1 cOmplete™ protease inhibitor cocktail EDTA free tablet) and protein concentrations determined using the DC protein assay (Bio-Rad, Hercules, CA). Oxygen Consumption Rate (OCR) is reported relative to protein content (pmol/min/µg). Estimations of ATP production derived from both oxidative phosphorylation and glycolysis were performed as previously described (18).

#### **Mitochondrial Membrane Potential**

Control and VDR-KD (n=5 wells/group) cells were plated at  $1.0 \times 10^5$  cells/well in 100 µl of growth medium in a black 96-well plate with a clear bottom (Corning, Costar, NY, USA). Cells were subsequently incubated for 30 minutes with 100 nM of tetramethylrhodamine ethyl ester (TRME). Following incubation cells were washed with PBS/0.2% BSA and then read at 549 nm using a CLARIOstar microplate reader (BMG Labtech, Germany) in 100 µl of PBS/0.2% BSA.

154

## 155 **Immunoblotting**

156 Control and VDR-KD (n=5-6 wells/group) cells were plated at  $1.0 \times 10^{10}$  cells/well in  
157 2 ml of growth medium in 6-well plates (Nunc, Roskilde, Denmark). Both myoblasts  
158 and myotubes were maintained and harvested as described previously, with protein  
159 concentrations determined using the DC protein assay (Bio-Rad, Hercules, CA).  
160 Total protein lysates of a known concentration were mixed 3:1 with 4x Laemmli  
161 sample loading buffer. Prior to gel loading, samples were boiled for 5 minutes unless  
162 probing for MitoProfile OXPHOS antibody cocktail, in which case non-denatured  
163 samples were used. The immunoblotting procedure was performed as previously  
164 described (27).

165

## 166 **Antibodies**

167 All primary antibodies were used at a concentration of 1:1000 in TBS-T. Antibody for  
168 dynamin-1-like protein (DRP1;8570) was from Cell Signaling Technology; MitoProfile  
169 OXPHOS antibody cocktail (110413) and mitofilin (110329) were from Abcam; Optic  
170 Atrophy-1/dynamin-like 120 kDa protein (OPA1; CPA3687) was from BD  
171 Biosciences; citrate synthase (CS; SAB2701077) and mitochondrial fission protein 1  
172 (FIS1; HPA017430) were from Sigma Aldrich; vitamin D receptor (D-6) (VDR; 13133)  
173 was from Santa Cruz Biotechnology. Secondary antibodies were used at a  
174 concentration of 1:10,000 in TBS-T. Anti-mouse (7076) and anti-rabbit (7074) were  
175 from Cell Signaling Technology.

176

## 177 **Statistical Analysis**

Statistical analysis was performed using the Statistical Package for the Social Sciences (SPSS) version 24.0. Differences between control and VDR-KD C2C12s were determined by independent t-tests. All data is presented as mean  $\pm$  standard deviation (SD). Statistical significance was set at  $P < 0.05$ .

## RESULTS

### Successful generation of VDR-KD myoblasts

Following shRNA interference, VDR protein content was reduced by 96% ( $P < 0.001$ ) and 95% ( $P < 0.001$ ) in VDR-KD C2C12 myoblasts (Fig. 1A) and myotubes (Fig. 1B) respectively.

### VDR-KD results in reduced mitochondrial respiration in C2C12 myoblasts and myotubes

In order to determine the effects of VDR-KD upon mitochondrial function, extracellular flux analysis was performed in VDR-KD myoblasts and myotubes. VDR-KD myoblasts displayed a 30% reduction in basal respiration compared to control ( $P = 0.034$ ; Fig. 2B). In addition, coupled and maximal respiration was reduced by 30% ( $P = 0.023$ ) and 36% ( $P = 0.013$ ) respectively. Furthermore, the spare respiratory capacity was also reduced by 39% ( $P = 0.008$ ; Fig 2.B). This deficit was retained following differentiation, with VDR-KD myotubes displaying a 34% reduction in basal respiration ( $P < 0.001$ ) and a 33% reduction in coupled respiration ( $P < 0.001$ ) (Fig. 2D). Furthermore, maximal respiration was reduced by 48% ( $P < 0.001$ ) and the spare respiratory capacity by 53% ( $P < 0.001$ ; Fig. 2D) in VDR-KD. Whilst proton leak remained unchanged in VDR-KD myoblasts (Fig. 2B), VDR-KD myotubes



displayed a 67% decrease in proton leak ( $P < 0.001$ ; Fig. 2D). To establish where mitochondrial impairments originated, we estimated oxidative phosphorylation ( $\text{ATP}_{\text{Ox}}$ ) and glycolysis ( $\text{ATP}_{\text{Glyc}}$ ) using recently described equations (18). Accordingly, total ATP production and  $\text{ATP}_{\text{Ox}}$  were reduced by 18% ( $P = 0.002$ ) and 20% ( $P = 0.007$ ) respectively in VDR-KD myoblasts (Fig. 2E). Finally, mitochondrial membrane potential assessed via TMRE fluorescence was reduced by 25% in VDR-KD ( $P = 0.001$ ; Fig. 2F).

### **No change in mitochondrial related protein content in VDR-KD myoblasts and myotubes.**

Given the observed decrements in mitochondrial respiration in both VDR-KD myoblasts and myotubes, we sought to determine whether a reduction in mitochondrial related protein content might underlie this phenotype. However, no differences were observed in mitochondrial ETC subunit I-V, citrate synthase (CS) or cytochrome c (Cyt c) protein content in either VDR-KD myoblasts (Fig. 3A) or myotubes (Fig. 3C). In order to further explore the potential influence of mitochondrial dynamics in mediating the observed decrements in mitochondrial function, multiple proxy markers of mitochondrial fusion and fission were probed. MFN2 remained unchanged although, OPA1 increased by 15% in both VDR-KD myoblasts ( $P = 0.021$ ; Fig. 4A) and myotubes ( $P = 0.046$ ; Fig. 4C). Furthermore, Mitofilin, FIS1 and DRP1 all remained unchanged in VDR-KD myoblasts (Fig. 4A) and myotubes (Fig. 4C).

## DISCUSSION

The role of vitamin D within skeletal muscle has received considerable interest in recent years, with current evidence suggesting that vitamin D related metabolites promote mitochondrial function within skeletal muscle (22-26). Building upon previous studies, we demonstrate that loss of VDR function results in significant reductions in mitochondrial respiration in both myoblasts and myotubes (Fig. 2A-D). Furthermore, we report that impairments were specifically observed in respiration derived from oxidative phosphorylation ( $\text{ATP}_{\text{Ox}}$ ) (Fig. 2E) and were not as a result of decreased mitochondrial related protein content (Fig. 3A-D).

Previously, it has been reported that mitochondrial protein content remains unchanged in both human skeletal muscle myoblasts treated with  $1\alpha,25(\text{OH})_2\text{D}_3$  and within the quadriceps of VDR-mKO mice (10, 23). Similarly, we also observed no change in mitochondrial protein content in both VDR-KD myoblasts and myotubes. Despite this, it has been reported that the treatment of both human primary and C2C12 myoblasts with vitamin D metabolites resulted in an increase in mitochondrial function (22, 23, 25). Whilst the observed increases in respiration were abolished following siRNA silencing of the VDR in human primary myoblasts (23), the role of the VDR in basal mitochondrial regulation is unknown. Therefore, our results build upon previous findings and indicate that the VDR is required for the maintenance of optimal mitochondrial respiration in myoblasts and myotubes. Furthermore, our results demonstrating that VDR-KD cells have significant reductions in  $\text{ATP}_{\text{Ox}}$ , suggesting that impairments are intrinsic to the mitochondria following VDR loss-of-function and are not mediated by decreases in mitochondrial protein content *per se*.

Despite *in vitro* evidence indicating vitamin D and the VDR regulate skeletal muscle mitochondrial function (22, 23, 25), *in vivo* evidence is currently lacking. Given that the supplementation of vitamin D has been shown to improve symptoms of fatigue and indirect measures of mitochondrial function (26), further examination of the role of vitamin D and the VDR *in vivo* is warranted.

The mitochondria exist in a reticulated network within skeletal muscle (28) and therefore, we also examined multiple markers of mitochondrial dynamics to ascertain whether loss of VDR function may alter mitochondrial morphology. Although we observed no differences in the abundance of MFN2, we did observe small but significant (~15%) increase in OPA1 protein abundance in both VDR-KD myoblasts and myotubes. OPA1 is known to modulate fusion of the inner mitochondrial membrane, cristae remodelling and reduce mitochondrial fragmentation in protection from apoptosis (5, 6, 8). Given the observed impairments in mitochondrial function and membrane potential following VDR-KD, an increase in OPA1 may be a compensatory mechanism to try and rescue mitochondrial dysfunction. Interestingly, OPA1 was also shown to be responsive to  $1\alpha,25(\text{OH})_2\text{D}_3$  treatment in human skeletal muscle myoblasts suggesting mitochondrial dynamics within skeletal muscle may be influenced by vitamin D status (23). Further examination of the mitochondrial network in VDR-KD cell lines via mitochondrial labelling techniques may shed light upon VitD-VDR-OPA1 interactions in this context.

In summary, we report a requirement for the VDR to maintain optimal mitochondrial respiration in C2C12 myoblasts and myotubes. The observed reductions in mitochondrial function were a result of reduced  $\text{ATP}_{\text{Ox}}$  although in contrast, markers

of mitochondrial protein content were unchanged. The regulatory role of the VDR within skeletal muscle mitochondrial function *in vivo* remains largely underexplored. Given the observed reduction in mitochondrial function *in vitro*, the examination of mitochondrial function within the skeletal muscle of VDR-mKO mice may reveal similar impairments in respiration (4, 10). Furthermore, it is possible that reductions in mitochondrial respiration may be linked to dysregulation of mitochondrial organisation, membrane permeability or calcium homeostasis. With regard to the latter, the treatment of skeletal muscle cell lines with vitamin D related metabolites has been shown to increase calcium flux (3, 19) however, this has not previously been linked to mitochondrial respiration. Overall, given the significant reduction in mitochondrial respiration displayed following VDR deletion, our results suggest that the VDR plays a fundamental regulatory role in skeletal muscle mitochondrial function.

303

304

305 **Grants**

306 The MRC-ARUK Centre for Musculoskeletal Ageing Research was funded through  
307 grants from the Medical Research Council [grant number MR/K00414X/1] and  
308 Arthritis Research UK [grant number 19891] awarded to the Universities of  
309 Birmingham and Nottingham. S.P.A. was funded by a MRC-ARUK Doctoral Training  
310 Partnership studentship, joint funded by the College of Life and Environmental  
311 Sciences, University of Birmingham.

312

313 **Disclosures**

314 No conflicts of interest, financial or otherwise, are declared by the authors.

315

316 **Author Contributions**

317 S.P.A and A.P conceived and designed research; J.J.B and A.A.K generated VDR-  
318 KD and control cell lines. S.P.A performed experiments, analysed data, interpreted  
319 results and prepared figures. S.P.A, J.J.B, P.J.A and A.P drafted the manuscript. All  
320 authors approved the final version of the manuscript.

321

## 322 REFERENCES

- 323 1. **Bhan A, Rao AD, and Rao DS.** Osteomalacia as a result of vitamin D deficiency.  
324 *Endocrinol Metab Clin North Am* 39: 321-331, table of contents, 2010.
- 325 2. **Bouillon R, and Verstuyf A.** Vitamin D, Mitochondria, and Muscle. *The Journal of*  
326 *Clinical Endocrinology & Metabolism* 98: 961-963, 2013.
- 327 3. **Buitrago CG, Arango NS, and Boland RL.** 1 $\alpha$ ,25(OH) $_2$ D $_3$ -dependent modulation  
328 of Akt in proliferating and differentiating C2C12 skeletal muscle cells. *J Cell Biochem* 113:  
329 1170-1181, 2012.
- 330 4. **Chen S, Villalta SA, and Agrawal DK.** FOXO1 Mediates Vitamin D Deficiency-Induced  
331 Insulin Resistance in Skeletal Muscle. *J Bone Miner Res* 31: 585-595, 2016.
- 332 5. **Cipolat S, Martins de Brito O, Dal Zilio B, and Scorrano L.** OPA1 requires mitofusin 1  
333 to promote mitochondrial fusion. *Proceedings of the National Academy of Sciences of the*  
334 *United States of America* 101: 15927-15932, 2004.
- 335 6. **Cogliati S, Frezza C, Soriano ME, Varanita T, Quintana-Cabrera R, Corrado M,**  
336 **Cipolat S, Costa V, Casarin A, Gomes LC, Perales-Clemente E, Salviati L, Fernandez-Silva P,**  
337 **Enriquez JA, and Scorrano L.** Mitochondrial cristae shape determines respiratory chain  
338 supercomplexes assembly and respiratory efficiency. *Cell* 155: 160-171, 2013.
- 339 7. **Forrest KY, and Stuhldreher WL.** Prevalence and correlates of vitamin D deficiency in  
340 US adults. *Nutr Res* 31: 48-54, 2011.
- 341 8. **Frezza C, Cipolat S, Martins de Brito O, Micaroni M, Beznoussenko GV, Rudka T,**  
342 **Bartoli D, Polishuck RS, Danial NN, De Strooper B, and Scorrano L.** OPA1 controls apoptotic  
343 cristae remodeling independently from mitochondrial fusion. *Cell* 126: 177-189, 2006.
- 344 9. **Girgis CM, Cha KM, Houweling PJ, Rao R, Mokbel N, Lin M, Clifton-Bligh RJ, and**  
345 **Gunton JE.** Vitamin D Receptor Ablation and Vitamin D Deficiency Result in Reduced Grip  
346 Strength, Altered Muscle Fibers, and Increased Myostatin in Mice. *Calcif Tissue Int* 97: 602-  
347 610, 2015.
- 348 10. **Girgis CM, Cha KM, So B, Tsang M, Chen J, Houweling PJ, Schindeler A, Stokes R,**  
349 **Swarbrick MM, Evesson FJ, Cooper ST, and Gunton JE.** Mice with myocyte deletion of  
350 vitamin D receptor have sarcopenia and impaired muscle function. *Journal of cachexia,*  
351 *sarcopenia and muscle* 2019.
- 352 11. **Girgis CM, Clifton-Bligh RJ, Mokbel N, Cheng K, and Gunton JE.** Vitamin D signaling  
353 regulates proliferation, differentiation, and myotube size in C2C12 skeletal muscle cells.  
354 *Endocrinology* 155: 347-357, 2014.
- 355 12. **Girgis CM, Mokbel N, Cha KM, Houweling PJ, Abboud M, Fraser DR, Mason RS,**  
356 **Clifton-Bligh RJ, and Gunton JE.** The vitamin D receptor (VDR) is expressed in skeletal  
357 muscle of male mice and modulates 25-hydroxyvitamin D (25OHD) uptake in myofibers.  
358 *Endocrinology* 155: 3227-3237, 2014.
- 359 13. **Ham AW, and Lewis MD.** Hypervitaminosis D Rickets: The Action of Vitamin D. *Br J*  
360 *Exp Pathol* 15: 228-234, 1934.
- 361 14. **Haussler MR, Whitfield GK, Kaneko I, Haussler CA, Hsieh D, Hsieh JC, and Jurutka**  
362 **PW.** Molecular mechanisms of vitamin D action. *Calcif Tissue Int* 92: 77-98, 2013.
- 363 15. **Holick MF, Binkley NC, Bischoff-Ferrari HA, Gordon CM, Hanley DA, Heaney RP,**  
364 **Murad MH, and Weaver CM.** Evaluation, treatment, and prevention of vitamin D deficiency:  
365 an Endocrine Society clinical practice guideline. *J Clin Endocrinol Metab* 96: 1911-1930,  
366 2011.

16. **Kazi AA, and Lang CH.** PRAS40 regulates protein synthesis and cell cycle in C2C12 myoblasts. *Mol Med* 16: 359-371, 2010.
17. **Mangelsdorf DJ, and Evans RM.** The RXR heterodimers and orphan receptors. *Cell* 83: 841-850, 1995.
18. **Mookerjee SA, Gerencser AA, Nicholls DG, and Brand MD.** Quantifying intracellular rates of glycolytic and oxidative ATP production and consumption using extracellular flux measurements. *J Biol Chem* 292: 7189-7207, 2017.
19. **Morelli S, de Boland AR, and Boland RL.** Generation of inositol phosphates, diacylglycerol and calcium fluxes in myoblasts treated with 1,25-dihydroxyvitamin D3. *The Biochemical journal* 289 ( Pt 3): 675-679, 1993.
20. **Owens DJ, Sharples AP, Polydorou I, Alwan N, Donovan T, Tang J, Fraser WD, Cooper RG, Morton JP, Stewart C, and Close GL.** A systems-based investigation into vitamin D and skeletal muscle repair, regeneration, and hypertrophy. *Am J Physiol Endocrinol Metab* 309: E1019-1031, 2015.
21. **Pike JW, Meyer MB, and Bishop KA.** Regulation of target gene expression by the vitamin D receptor - an update on mechanisms. *Rev Endocr Metab Disord* 13: 45-55, 2012.
22. **Romeu Montenegro K, Maron Carlessi R, Fernandes Cruzat V, and Newsholme P.** Effects of vitamin D on primary human skeletal muscle cell proliferation, differentiation, protein synthesis and bioenergetics. *The Journal of steroid biochemistry and molecular biology* 105423, 2019.
23. **Ryan ZC, Craig TA, Folmes CD, Wang X, Lanza IR, Schaible NS, Salisbury JL, Nair KS, Terzic A, Sieck GC, and Kumar R.** 1 $\alpha$ ,25-Dihydroxyvitamin D3 Regulates Mitochondrial Oxygen Consumption and Dynamics in Human Skeletal Muscle Cells. *J Biol Chem* 291: 1514-1528, 2016.
24. **Ryan ZC, Craig TA, Wang X, Delmotte P, Salisbury JL, Lanza IR, Sieck GC, and Kumar R.** 1 $\alpha$ ,25-dihydroxyvitamin D3 mitigates cancer cell mediated mitochondrial dysfunction in human skeletal muscle cells. *Biochem Biophys Res Commun* 496: 746-752, 2018.
25. **Schnell DM, Walton RG, Vekaria HJ, Sullivan PG, Bollinger LM, Peterson CA, and Thomas DT.** Vitamin D produces a perilipin 2-dependent increase in mitochondrial function in C2C12 myotubes. *J Nutr Biochem* 65: 83-92, 2018.
26. **Sinha A, Hollingsworth KG, Ball S, and Cheetham T.** Improving the vitamin D status of vitamin D deficient adults is associated with improved mitochondrial oxidative function in skeletal muscle. *J Clin Endocrinol Metab* 98: E509-513, 2013.
27. **Stocks B, Dent JR, Joannis S, McCurdy CE, and Philp A.** Skeletal Muscle Fibre-Specific Knockout of p53 Does Not Reduce Mitochondrial Content or Enzyme Activity. *Frontiers in physiology* 8: 941-941, 2017.
28. **Westermann B.** Bioenergetic role of mitochondrial fusion and fission. *Biochimica et Biophysica Acta (BBA) - Bioenergetics* 1817: 1833-1838, 2012.

## Figure Legends

### **Figure 1. Generation of Vitamin D Receptor (VDR) loss of function C2C12**

**myoblasts.** A: Quantification of VDR protein content in VDR-KD compared to control myoblasts and myotubes. B: Representative immunoblot images of VDR protein content in VDR-KD myoblasts and myotubes.  $^{**}P < 0.005$ , independent t-test. Data mean  $\pm$  SD (n=5-6 lanes/group) and represented as a fold change from control.

### **Figure 2. VDR-KD myoblasts display reduced mitochondrial respiration**

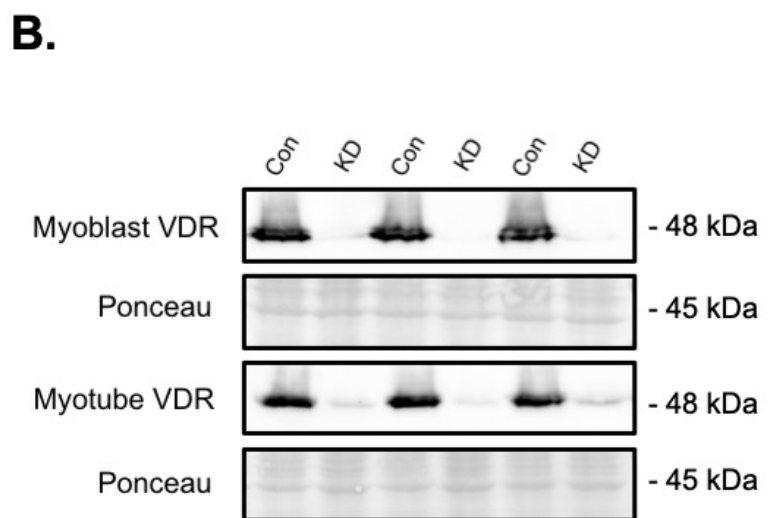
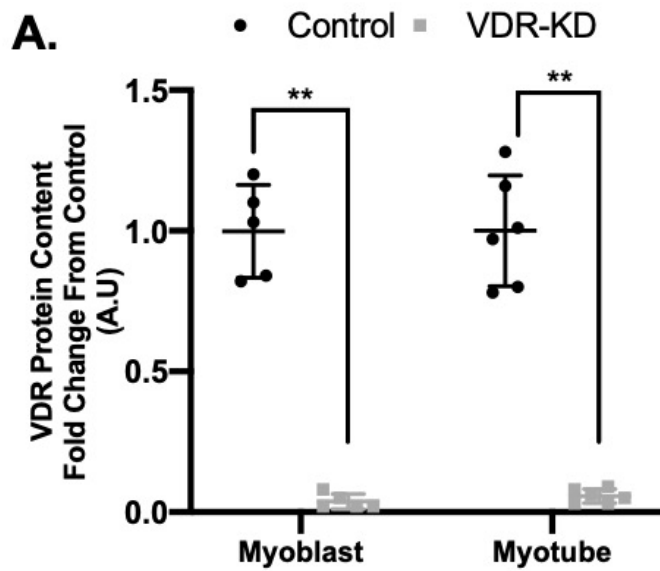
**compared to control.** A: Oxygen consumption rate (OCR) during analysis of respiratory control in control and VDR-KD myoblasts. B: Respiratory control parameters from control and VDR-KD myoblasts. C: OCR during analysis of respiratory control in control and VDR-KD myotubes. D: Respiratory control parameters from control and VDR-KD myotubes. E: Estimations of total ATP production (ATP<sub>Total</sub>), oxidative phosphorylation (ATP<sub>Ox</sub>) and glycolysis (ATP<sub>Glyc</sub>) in control and VDR-KD myoblasts. F: Mitochondrial membrane potential assessed via TMRE fluorescence in control and VDR-KD myoblasts.  $^{**}P < 0.05$ ,  $^{**}P < 0.005$ , independent t-test. Data mean  $\pm$  SD (A-E: n=9-10 wells/group. F: n=5 wells/group).

### **Figure 3. No change in markers of mitochondrial protein content in VDR-KD**

**myoblasts compared to control.** A: Protein abundance of mitochondrial subunits complex I (NDUFB8), complex II (SDHB), complex IV (MTCO1), complex V (ATP5A) as well as citrate synthase (CS) and cytochrome c (Cyt c) in control and VDR-KD myoblasts. Data mean  $\pm$  SD (n=6 lanes/group) and represented as a fold change from control.

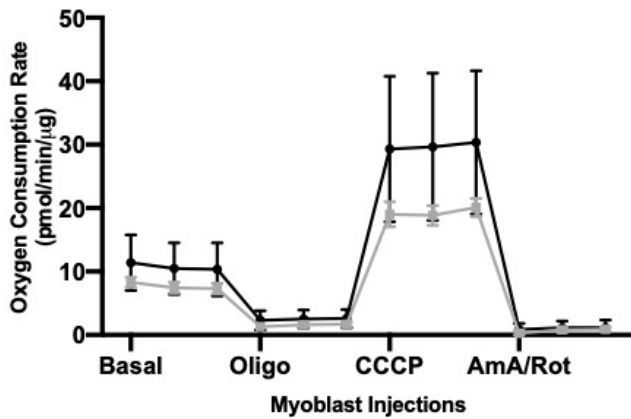


**Figure 4. Markers of mitochondrial fission remain unchanged whilst OPA1 protein abundance is increased in VDR-KD myoblasts compared to control. A:** Protein abundance of markers of mitochondrial fusion (MFN2 and OPA1) and fission (Mitofilin, Fis1 and DRP1). \* $P < 0.05$ , independent t-tests. Data mean  $\pm$  SD (n=6 lanes/group) and represented as a fold change from control.

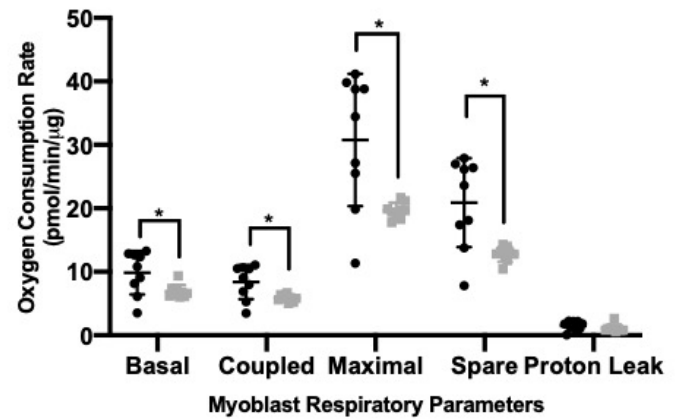


• Control    ■ VDR-KD

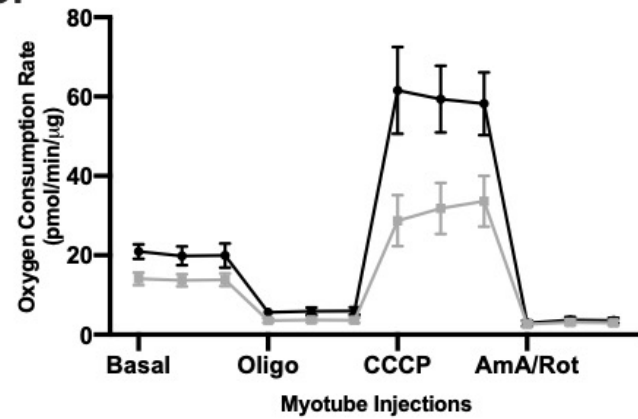
**A.**



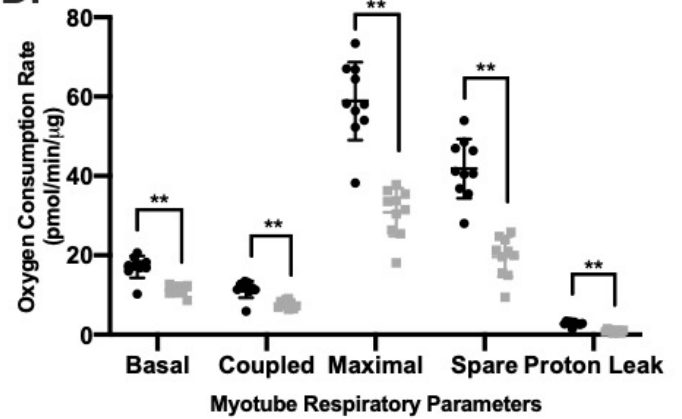
**B.**



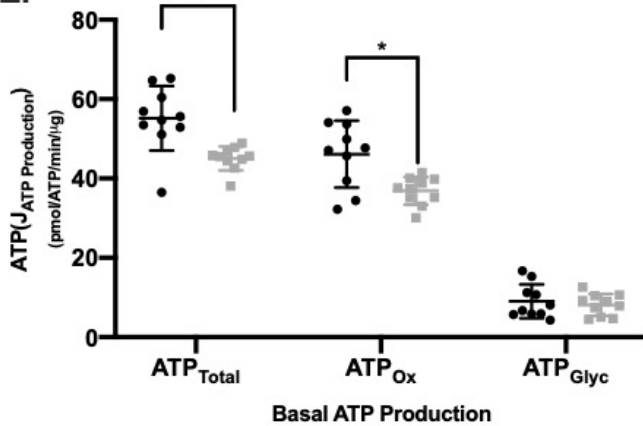
**C.**



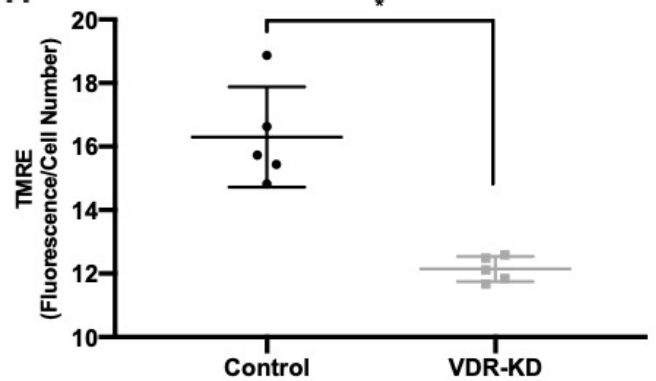
**D.**

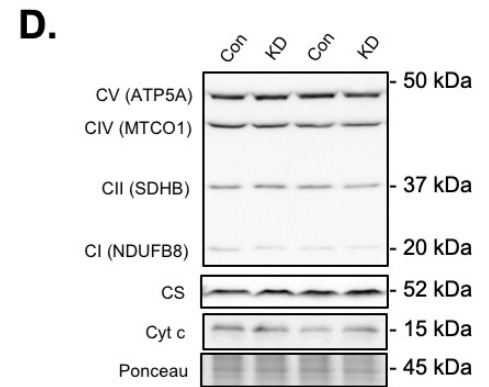
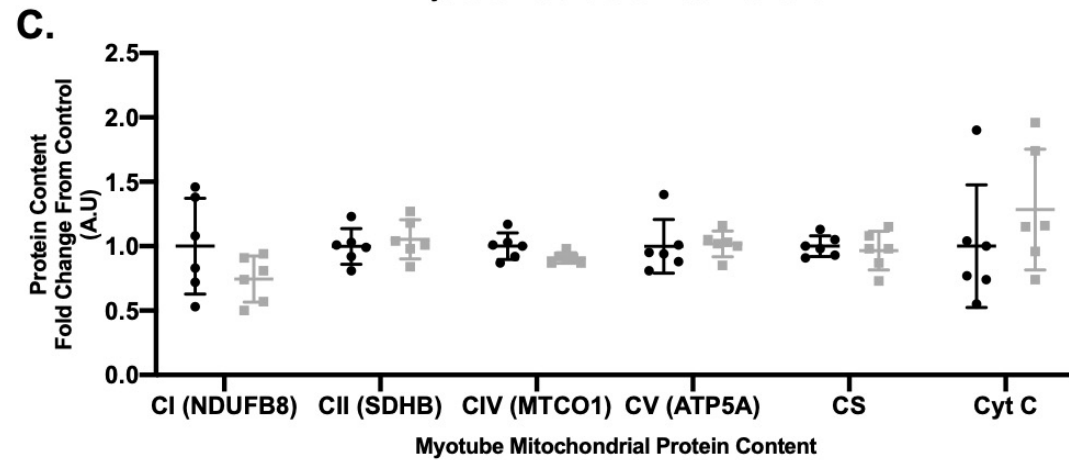
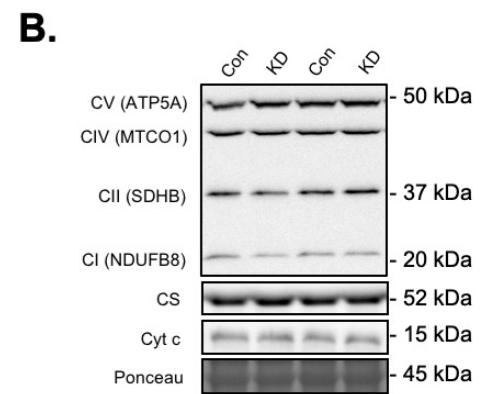
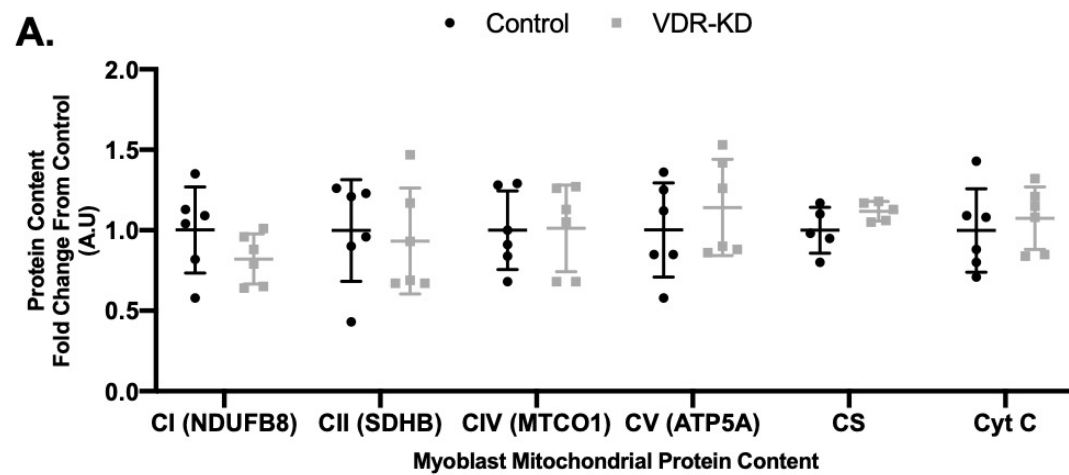


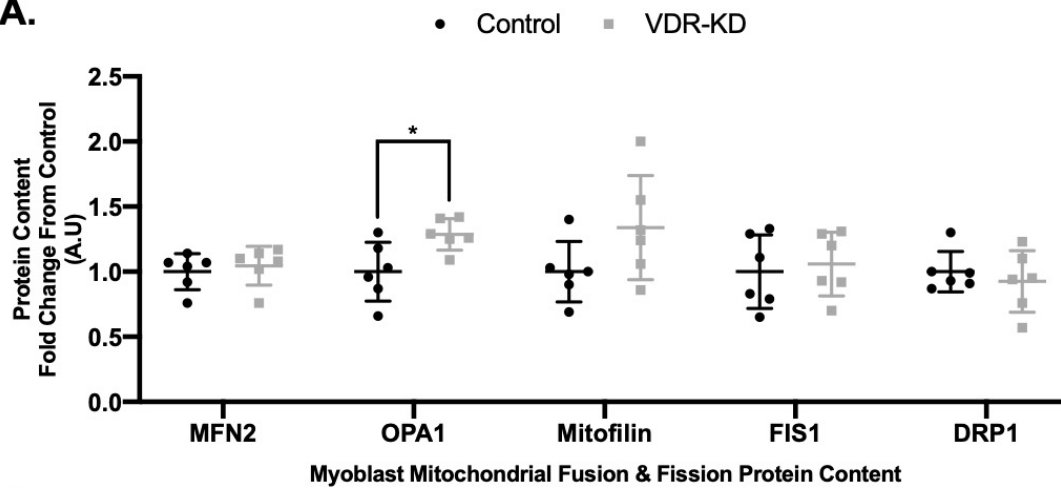
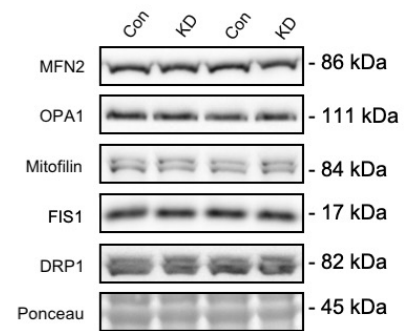
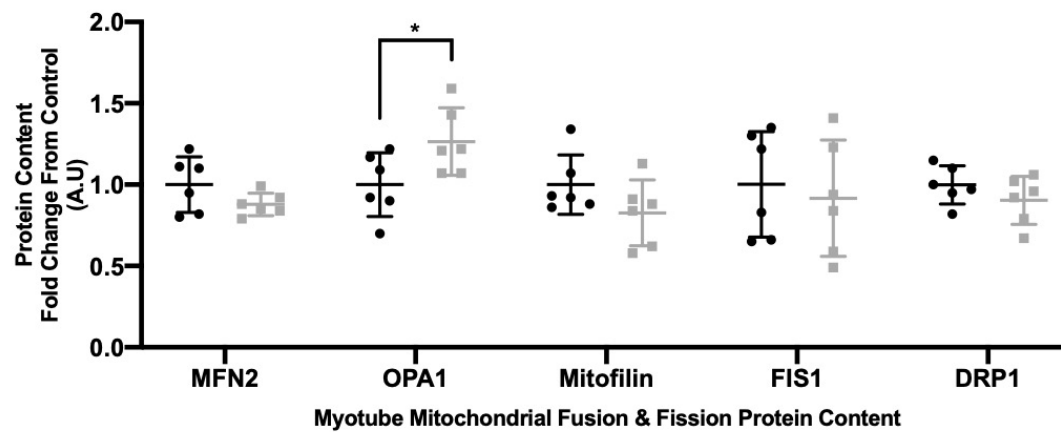
**E.**



**F.**





**A.****B.****C.****D.**